J. Nano- Electron. Phys.
3 (2011) No1, P. 1071-1080

© 2011 SumDU
(Sumy State University)

PACS numbers: 73.61.Ey,73.50.Bk,72.10._d

MODELING OF ELECTRON MOBILITY OF GaN AT LOW TEMPERATURE AND LOW ELECTRIC FIELD

Souradeep Chakrabarti, Shyamasree Gupta Chatterjee, Somnath Chatterjee

Techno India Salt Lake,
EM 4/1, Salt Lake, Kolkata – 700091
E-mail: souradeep100@yahoo.co.in

An analytical model at low temperature and low field electron mobility of GaN *has been developed. The electron mobility in* GaN *have been calculated using Relaxation Time Approximation method considering elastic process of acoustic phonon deformation potential scattering, acoustic piezoelectric scattering and ionized impurity scattering, neutral impurity scattering, dislocation scattering. Ionized impurity scattering has been treated beyond the Born approximation using Dingle and Brooks- Herring analysis. The compensation ratio is used as a parameter with a realistic charge neutrality condition. Degeneracy is very important factor as it is used to imply different statistics (Maxwell – Boltzmann or Fermi – Dirac) at different temperature. Generalized M-B statistics are used throughout because the samples we have used to compare our results are highly Non-degenarate. The result shows that, the proposed model can accurately predict the electron mobility as a function of both the carrier concentration and the temperature upto* 200 *K. The discrepancy of this model above temperature* 200 *K presumably results from the following factors: ignoring the role of optical phonon, at low temperature consideration of parabolic band i.e. neglecting the effect of inter-velly scattering and ignoring the effect of very few interfacial charges in the degenerate layer at the* GaN*-substrate interface.*

Keywords: *MODELING OF ELECTRON MOBILITY, M-B STATISTICS, DEGENERACY, LOW TEMPERATURE, ELASTIC SCATTERINGS, ACOUSTIC PHONON DEFORMATION POTENTIAL, ACOUSTIC PHONON PIEZOELECTRIC, IONIZED IMPURITY, DISLOCATION SCATTERING, NEUTRAL IMPURITY.*

(Received 04 February 2011)

1. INTRODUCTION

GaN is one of the principal materials used for a number of optoelectronic and electronic devices including laser diodes [1], light-emitting diodes [2], photo detectors [3], metal semiconductor field-effect transistors (MESFETs) [4], high electron mobility transistors (HEMTs) [5] and hetero junction bipolar transistors (HBTs) [6]. For these devices, high electron mobility is a prerequisite for achieving high performance. The importance of GaN may be due to its relatively large band gap (3.4 eV), strong bond strength (2.3 eV/bond) and high breakdown voltage ($3 \cdot 10^6$ V/cm).

The electron mobility is the most popular and important transport parameter used to characterize conductivity tensor. Mobility is considered to be the *figure of merit* for materials used for electronic devices. Determination of fundamental material parameters and understanding of electron scattering mechanisms demand accurate comparison between experiment and theory.

GaN is normally grown by molecular beam epitaxy (MBE), metal-organic chemical vapor deposition (MOCVD) or hybrid vapor phase epitaxy (HVPE) on a substrate like; grown on sapphire substrates, which causes lattice mismatch at the interface. This mismatch generates highly dislocated and defective region to relieve the strain [cks].

GaN is usually crystallizes in the wurtzite lattice (also known as hexagonal or α-GaN). However, under certain conditions, zincblend GaN (sometimes referred to as cubic or β-GaN) can also be grown. At ambient conditions, the thermodynamically stable phase is wurtzite for bulk GaN. The cohesive energy per bond in wurtzite variety is 2.20 eV (48.5 kcal/mol) GaN [8]. Although the calculated energy difference between wurtzite and zincblende lattice is small (− 9.88 meV/atom for GaN), the wurtzite form is energetically preferable due to its stability.

The mobility of GaN has been investigated by several groups [9-14]. Look et al. [10] and Look and Molnar [11] developed a two-layer model for the electron mobility. In their model, data were fitted by solving the Boltzmann equation in the relaxation time approximation. But polar optic phonon scattering has been used in low temperature also, though it has very less impact at low temperature.

Among the three conduction bands of the wurtzite-GaN, for our modeling we have used the parabolic one because the samples are wide − band gap and bulk structure.

In GaN, above nearly 200 K temperature, the dominant scattering mechanism is the polar optic phonon scattering mechanism [15, Dhar]. In the present work, numerical modeling of the electron mobility at low field and low temperature as a function of temperature and electron concentration for wurtzite GaN are carried out using the relaxation time approximation method for elastic scattering processes including acoustic phonon scattering (with the two modes deformation potential and piezoelectric), neutral impurity scattering, dislocation scattering and ionized impurity scattering. To find out the mobility at different temperatures with different concentration programs have been written on MATLAB. The objective of this paper is to model the electron mobility in GaN at low temperature (upto ~ 200 K) without using the polar optic phonon scattering.

1.1 Model

In this work, we have reported on an analytical model for the temperature and concentration-dependent electron mobility of GaN. In this model, scatterings by ionized impurities, acoustic phonons, neutral impurity and dislocations have been considered to analyze the experimental behavior of mobility for GaN device.

The concentration of electron is not constant. It varies with the change of temperature, and with the change of doping concentration.

The presence of a dopant impurity creates a bound level E_d near the conduction band edge. We note that carrier densities the electrons will be redistributed, but their numbers will be conserved and will satisfy the following equality resulting from charge neutrality condition.

To calculate densities of electrons at finite temperatures in doped semiconductors,

$$n + n_d = N_d$$

Where, n = total free electrons in the conduction band, n_d = electrons bound to the donors

$$\frac{n}{n+n_d}=\frac{1}{1+\dfrac{N_c}{2N_d}\exp\left(-\dfrac{E_c-E_d}{kT}\right)} \tag{1}$$

$$N_c=2\left(\frac{2\pi m_e kT}{h^2}\right)^{2/3} \tag{2}$$

The factor 1/2 essentially arises from the fact that there are two states an electron can occupy at a donor site corresponding to the two spin-states. N_c = is the density of states at Energy level "E"

$$E_d=E_c-13.6\frac{m^*}{m_0}\left(\frac{\varepsilon_0}{\varepsilon}\right)^2 eV\,, \tag{3}$$

where E_c = conduction band energy, ε_0 = permittivity of vacuum, ε_0 = permittivity of donor, m^* = effective mass, m_0 = rest mass of electron [24].

Now the Fermi level has been calculated using the following equations to determine the degeneracy of samples on the basis of electron concentration and temperature. Degeneracy is very important factor as it is used to imply different statistics (Maxwell-Boltzmann or Fermi-Dirac) at different temperature. Generalized M-B statistics are used throughout because the samples we have used to compare our results are highly Non-degenerate.

We shall now introduce a spherical coordinate system with the k direction as the polar axis. In this system let (k', β, Φ) be the spherical coordinates of k', the azimuthal angle Φ being measured from the k-ε plane Fig. 1. One may then write [25]

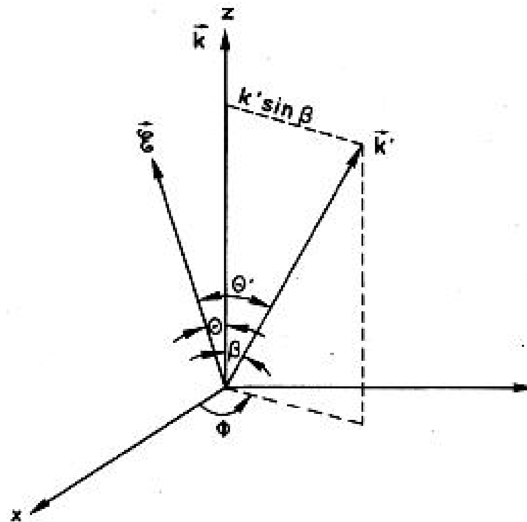

Fig. 1 *– spherical coordinate system with the k direction as the polar axis [ref-25]*

$$n = \int \frac{2}{(2\pi)^3} f dk \tag{4}$$

$$k = \sqrt{2m^* E}/h' \tag{5}$$

$$dk' = k'^2 dk' \sin \beta d_{\beta d\phi} \tag{6}$$

From this we derived

$$n = \int_{E_c}^{\alpha} \frac{(2m^* k_\beta T)^{3/2}}{2\pi^2 h'^3} F_{1/2}(\eta) \tag{7}$$

Where,

$$F_{1/2}(\eta) = \frac{E^{1/2} dE}{1 + \exp\left(\frac{E - E_F}{k_B T}\right)} \tag{8}$$

Where,

$$\eta = \left(E_F - E_C\right)/k_B T \tag{9}$$

Here, the electron mobility considering various elastic scattering mechanisms is determined by solving Boltzmann transport equation using the relaxation time approximation method. The parameter for characterizing the various scattering mechanisms is the relaxation time μ, which determines the rate of change in electron momentum as it moves through the semiconductor crystal. Mobility is related to the scattering time by

$$\mu = e\langle\tau\rangle/m^* \tag{10}$$

where τ is the average relaxation time over the electron energies and μ is the mobility, and m is the effective mass of electron. In the following sections, the expressions of relaxation time and mobility caused by different scattering mechanisms have been given.

2. ELECTRON MOBILITY

2.1 Phonon scatte

2.1.1 Deformation Potential Scattering

The acoustic mode lattice vibration induced changes in lattice spacing, which change the bandgap from point to point. Since the crystal is 'deformed' at these points, the potential is called the deformation potential. The corresponding scattering relaxation time can be written as

$$\tau(E) = \frac{\pi d h^4 V_S^2}{\sqrt{2} E_1^2 m^{*3/2} k_B T} E^{-1/2} \tag{11}$$

Where, $C_l = dV_s{}^2$; acoustic longitudinal elastic constant, V_s = average velocity of sound in GaN, d = mass density of GaN, E_1 = Acoustic deformation potential.

2.1.2 Piezoelectric Scattering

Electrons can suffer scattering with piezoelectric mode of acoustic lattice vibrations. In this scattering mechanism.The relaxation time due to piezoelectric potential scattering is given by

$$\tau(E) = \frac{2\sqrt{2}\pi h'^2 \varepsilon E^{1/2}}{e^2 p^2 m^{*1/2}(k_B T)}, \tag{12}$$

where $p = [hpz^2/dV_S{}^2\varepsilon]$ is the piezoelectric coupling coefficient, hpz = piezoelectric constant.

2.2 Impurity Scattering

2.2.1 Ionized Impurity Scattering

The amount of scattering due to electrostatic forces between the carrier and the ionized impurity depends on the interaction time and the number of impurities. Larger impurity concentrations result in a lower mobility [8]. The relaxation time due to scattering of ionized impurities is given by

$$\frac{1}{\tau(E)} = \frac{NZ^2 e^4}{16\sqrt{2}\pi\varepsilon^2 m^{*1/2}} E^{-3/2} \left(m(1+b) - \frac{b}{(1+b)} \right) \tag{13}$$

where
$$b = \frac{4k^2}{\beta_s^2} = \frac{8m^* E}{h'^2 \beta_s^2},$$

β_s is the inverse screening length

$$\beta_s^2 = \frac{ne^2}{\varepsilon k_B T} \frac{F_{-1/2}(\eta)}{F_{1/2}(\eta)},$$

N = ionized impurity which is for a sample with dislocation density and un-compensation is $N = n + f(N_s/d)$, N_s = dislocation density, d = c-lattice constant of a hexagonal GaN lattice, f = fraction of filled traps. For compensated $N = N_d^+ + N_a^-$, where N_d and N_a are donor and acceptor concentration

2.2.2 Neutral Impurity Scattering

When an electron passes close to neutral atom, momentum can be transferred through a process in which the free electron exchanges with a bound electron on the atom. The relaxation time can be written as

$$\tau(E) = \frac{m^*}{20 N_n h' a_0} \tag{14}$$

Where, a_0 is the effective Bohr radius of donor, and N_n is the concentration of neutral impurities.

2.3 Dislocation Scattering

The high density of dislocations and native defects induced by nitrogen vacancies in GaN, dislocation scattering and scattering through nitrogen vacancies has also been considered as a possible scattering mechanism. Dislocation scattering is due to the fact that acceptor centers are introduced along the dislocation line, which capture electrons from the conduction band in an n-type semiconductor. The dislocation lines become negatively charged and a space-charge region is formed around it, which scatters electrons traveling across the dislocations, thus reducing the mobility. The relaxation time is

$$\tau(E) = \frac{8(\varepsilon\varepsilon_0)^2 a^2 m^{*2}}{Ne^4 f^2 L_D}\left(V_t^2 + \frac{h'^2}{4m^{*2}L_D^2}\right)^{3/2} \quad (15)$$

Where V_t is the component of V perpendicular to dislocation line, a is the distance between imperfection centers along the dislocation line, and f is their occupation probability

3. ANALYSIS AND DISCUSSION

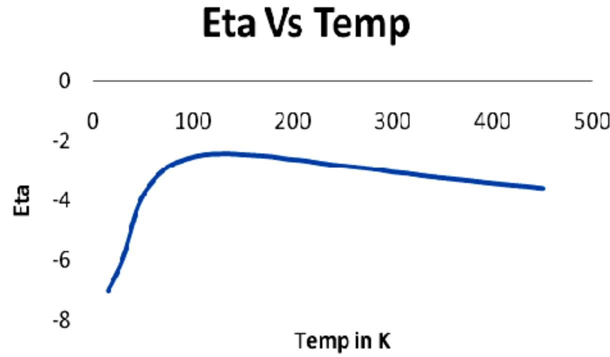

***Fig. 2** – The variation of Eta with temperature in the sample from ref-*26

The Fig. 1 shows the change in position of Fermi energy** with the temperature as well as electron concentrations has been plotted to observe the level of degeneracy for bulk- GaN sample from Refs 26. (Fig. 1)The sample is unintentionally doped and uncompensated n-type and grown by MOCVD technique. Fermi level has been calculated using equation 8 to determine the degeneracy of sample. It is prominent from figure that the sample we have used to compare our theoretical model is highly non-degenerate, therefore Generalized M-B statistics was used throughout.

(** Fermi level = $\eta k_B T + E_c$, where E_c is conduction band energy level.)

It is clear from Fig. 2 that in the case of sample from Refs. 26 electron concentrations increase with temperature and Above 100 K it gradually saturates [15].

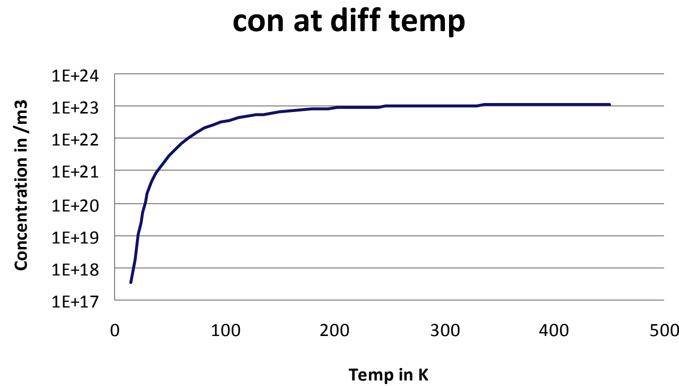

Fig. 3 – *The change of electron concentration at different temperature of the sample from ref-26*

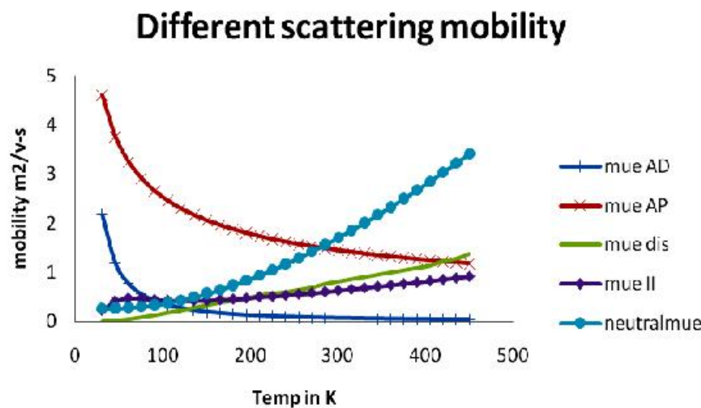

Fig. 4 – *Change of mobility for different scatterings at different temperatures*

Fig. 3 represents the variation of electron mobility with temperature for various types of scattering mechanism such as elastic process of acoustic phonon deformation potential scattering, acoustic piezoelectric scattering, ionized impurity scattering, neutral impurity scattering and dislocation scattering individually using the parameters of uncompensated n-type GaN. The measured values, shown in Table I, for the MOCVD sample is used for theoretical calculations. Here, the dislocation density, estimated by our model is $9 \times 10^{8}\text{cm}^{-2}$, Average longitudinal elastic constant, $C11$ is 1.85×10^{10} N/m^2 respectively. In n-type GaN the activation energy of the donors is quite large, which keeps a large number of donors neutral at low temperatures from 15 K to 60 K. Between 60 K to 100 larger impurities concentrations result in a lower mobility and Beyond 100 K almost all impurity atoms are ionized and Drift velocity of carriers become dominant [7].

From the graph it is seen that the electron mobility due to scattering by dislocations should increase monotonically with net carrier concentration, which satisfies with what is told by H.M. Ng, D. Doppalapudi, and T.D. Moustakas [Ref. 14].

It is found that f, the fraction of the filled traps increases with the increase of carrier concentration and dislocation density. For a constant dislocation density, f increases with T to a maximum, then decreases.

This behavior can be attributed to the competition between two opposing effects. First, the increase in temperature increases the number of free electrons, which leads to increasing f. Second, the increase in temperature provides energy for the electrons to escape from the traps, and this reduces f, it agrees well with our theoretical modeling.

Table 1 – *Sample parameters*

sample	Concentration at 300 K (cm^{-3})	Activation energy
RK-120c	1.03×10^{17}	13.5 eV

Table 2 – *Sample parameters used during simulation*

Parameter	Value
Displacement of the edge of the band per unit dilation of the lattice (acoustic deformation potential), E_{ds}	9.2 eV
Low-frequency relative dielectric constant,	8.9
Effective mass, m^*	$0.2m_0kg$
Lattice constant of the hexagonal lattice, d	5.185
Average longitudinal elastic constant, $C11$.	$1.85 \times 10^{10}\ N/m^2$

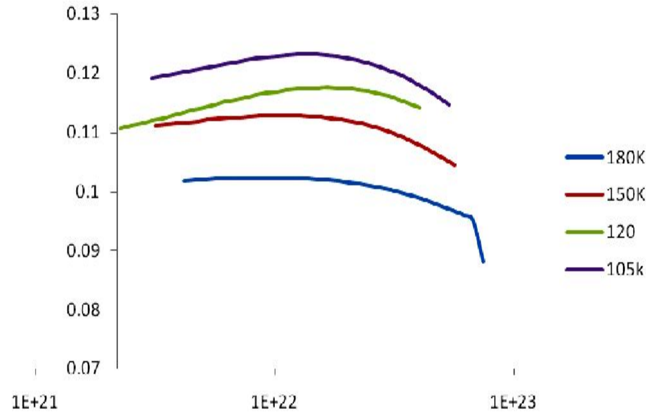

Fig 5 – *Mobilities in the range* 120-180 K

Fig. 4 shows the calculated electron drift mobilities as a function of carrier concentrations at 105 K and 150 K. As temperature increases the peak value of mobility decreases. We further note that the calculated drift mobilities shown in Fig. 3 are in good agreement with the values calculated using the iterative method and with recent MCSs [27]

It should be noted from Fig. 5 that GaN exhibits maximum mobilities in the range 120-180 K depending on the electron density [28]. This behavior is related to the interplay of acoustic phonon scattering at low carrier concentrations and ionized – impurity scattering at higher carrier concentrations. Also, the mobility is affected over the whole temperature range from 40 to 400 K, due to the presence of the interfacial layer. This interfacial layer causes lattice mismatch at the interface. This mismatch

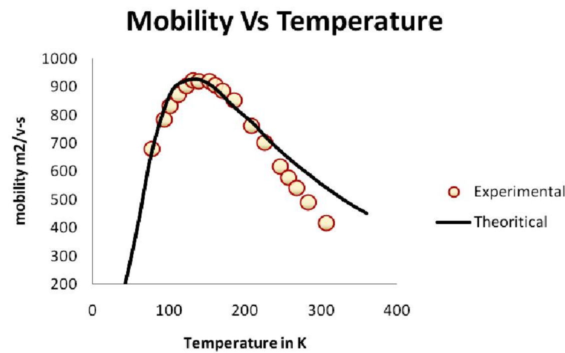

Fig. 6 *– Mobility variation at different temperatures*

generates highly dislocated and defective region to relieve the strain. This thin interface layer acts as a parallel degenerate conduction channel to the conduction in the bulk GaN layer. Our modeling suited well with the experimental data at low temperature (~ upto 210 K), but there is a deviation between our theoretical value and experimental data. This deviation can be well justified by the effect of polar optical phonon scattering. After 200 K at high temperature the inelastic polar optical phonon scattering, ,plasmon scattering will start affecting the electron mobility highly. Optical phonon scattering becomes dominant near after 200 K,which is the reason of sharper fall of the experimental data after 200 K.

4. CONCLUSION

In conclusion, a sufficiently accurate model for the electron mobility at low temperature and low electric field in GaN has been developed. The model has considered the scattering due to ionized impurities, dislocations and acoustic phonons. The model has shown that it can predict accurately the mobility at different doping concentrations and temperatures. The polar optic phonon has not been considered as of its low impact at low temperature. It is shown that upto 210 K an accurate model can be given for electron mobility in GaN without using polar optical phonon scattering.

REFERENCES

1. S. Nakamura, M. Senoh, S. Nagahama, N. Iwasa, T. Yamada, T. Matsushita, H. Kiyoku, Y. Sugimoto, *Jpn. J. Appl. Phys*. **35**, L217 (1996)
2. D. Steigerwald, S. Rudaz, H. Liu, R.S. Kern, W. Götz, R. Fletcher, *JOM-J. Min. Met. Mat. S.* **49**, 18 (1997).
3. J.M.V. Hove, R. Hickman, J.J. Klassseen, P.P. Chow, P.P. Ruden, *Appl. Phys. Lett.* **70**, 2282 (1997)
4. P. Klein, J. Freitas, Jr., S. Binari, *Appl. Phys. Lett*. **75**, 4016 (1999)
5. S. Sheppard, K. Doverspike, W. Pribble, S. Allen, J. Palmour, L. Kehias, T. Jenkins, *IEEE Electr. Device L*. **20**, 161 (1999)
6. L.S. McCarthy, P. Kozodoy, M.J.W. Rodwell, S. DenBaars, U. Mishra, *IEEE Electr. Device L*. **20**, 277 (1999)
7. K. Alfaramawi, *Journal of King Saud University – Science*, In press (2010)
8. D.L. Rode, D.K. Gaskill, *Appl. Phys. Lett*. **66**, 1972 (1995)

9. D.C. Look, D.C. Reynolds, J.W. Hemsky, J.R. Sizelove, R.L. Jones, R.J. Molnar, *Phys. Rev. Lett.* **79,** 2273 (1997)
10. D.C. Look, R.J. Molnar, *Appl. Phys. Lett.* **70,** 3377 (1997)
11. D.C. Look, J.R. Sizelove, *Phys. Rev. Lett.* **82,** 1237 (1999)
12. N.G. Weimann, L.F. Eastman, D. Doppalapudi, H.M. Ng, T.D. Moustakas , *J. Appl. Phys.* **83,** 3656 (1998)
13. H.M. Ng, D. Doppalapudi, T. Moustakas, N. Weimann, L. Eastman, *Appl. Phys. Lett.* **73,** 821 (1998)
14. S. Dhar, S. Ghosh, *J. Appl. Phys.* **86,** 2668 (1999)
15. J. Neugebaur, C.G. Van de Walle, *Phys. Rev. B* **50,** 8067 (1994)
16. H.P. Maruska, J.J. Tietjen, *Appl. Phys. Lett.* **15,** 327 (1969)
17. P. Perlin, T. Suski, H. Teisseyre, M. Leszczynski, I. Grzegory, J. Jun, S. Porowski, P. Bogusławski, J. Bernholc, J.C. Chervin, A. Polian, T.D. Moustakas, *Phys. Rev. Lett.* **75,** 296 (1995)
18. P. Boguslawski, E.L. Briggs, J. Bernholc, *Phys. Rev. B* **51,** 17255 (1995)
19. V.A. Gubanov, Z.W. Lu, B.M. Klein, C.Y. Fong, *Phys. Rev.* B **53,** 4377 (1996)
20. T. Mattila, A.P. Seitsonen, R.M. Nieminen, *Phys. Rev. B* **54,** 1474 (1996)
21. T. Mattila, R.M. Nieminen, *Phys. Rev. B* **55,** 9571 (1997)
22. D.J. Chadi, *Appl. Phys. Lett.* **71,** 2970 (1997)
23. U.K. Mishra, J. Singh *Semiconductor device physics and design*, (Springer)
24. D. Chattopadhya, H.J. Queisser, *Rev. Mod. Phys.* **53,** 745 (1981)
25. I.M. Abdel-Motaleb, Y.R. Korotkov, *J. Appl. Phys.* **97,** 093715 (2005)
26. V.W.L. Chin, T.L. Tansley, T. Osotchan, *J. Appl. Phys.* **75,** 7365 (1994).
27. S.O. Kasap, P. Capper, *Handbook of Electronic and Photonic Materials* (Springer).